

PRELIMINARY RESULTS OF NEW 50 MHz DOPPLER RADAR EXPERIMENT AT SYOWA STATION

Tadahiko OGAWA,

*Hiraiso Branch, Radio Research Laboratories, 3601 Isozaki,
Nakaminato-shi, Ibaraki 311-12*

Kiyoshi IGARASHI, Masami OSE, Yasukazu KURATANI,

*Radio Research Laboratories, 2-1, Nukui-Kitamachi 4-chome,
Koganei-shi, Tokyo 184*

Ryoichi FUJII and Takeo HIRASAWA

National Institute of Polar Research, 9-10, Kaga 1-chome, Itabashi-ku, Tokyo 173

Abstract: A 50 MHz doppler radar newly installed at Syowa Station in 1982 is characterized by the narrow antenna beams (4° in the horizontal plane) in two different directions (approximately geomagnetic and geographic south), the three operation modes (spectrum, double-pulse and meteor mode) and the minicomputer for both real time data processing and radar control. This paper aims to check up many functions given to the radar system by presenting some preliminary results obtained at a very early stage of its operation. It is confirmed that the radar and computer systems operate as planned and are useful for continuous monitoring of the lower auroral ionosphere in the 80–120 km height region.

1. Introduction

The newly developed 50 MHz doppler radar was installed at Syowa Station in February 1982 and now is in full operation for the Middle Atmosphere Program (MAP, 1982–1985) in Antarctica. This radar was designed to measure the intensity and doppler velocity of auroral radar echoes due to the 3-m irregularities appearing often in the disturbed *E*-region and also to detect the meteor echoes at the 80–110 km altitudes. An on-line minicomputer is used for both the radar system control and real time processing of a great deal of data with high spatial and time resolutions.

The system is very unique in its operation mode. There are three modes; spectrum, double-pulse and meteor mode, one of which an operator can select depending on the objectives of study. The spectrum mode gives doppler spectra of echoes from which some characteristics of the plasma turbulence during an auroral activity can be investigated (*e. g.*, OGAWA and IGARASHI, 1982). Mean doppler velocities of the irregularities are derived from the double-pulse mode. The electron drift (Hall drift) velocity determined by this mode can be ultimately related to the ionospheric electric field relying on the instability theories giving rise to 3-m irregularities (GREENWALD *et al.*, 1978; OGAWA *et al.*, 1982). In the meteor mode, neutral wind motions at the 80–110

km altitudes are investigated by using meteor trail as a tracer. Recently, it has been suggested that the auroral activity affects the mesospheric wind pattern (BALSLEY *et al.*, 1982) and that there is a relatively large discrepancy between the observed and the theoretical meridional winds (NASTROM *et al.*, 1982). Such problems may be solved in part by the present meteor mode. See a paper of IGARASHI *et al.* (1982) for detailed descriptions of the radar and computer systems and of the data processing procedures.

This paper presents very preliminary results obtained at an early stage of the experiment, from which it can be confirmed that the constructed radar and computer systems operate as planned and will be very useful for monitoring continuously the auroral ionosphere dynamics.

2. Configuration of Antennas

The new radar has the antenna beams toward both geomagnetic (GMS) and approximately geographic south (GGS) to investigate a two-dimensional structure of *E*-region irregularities or neutral wind motions. Figure 1 illustrates the plan view of the two antenna beams (crossing angle of 31.4°) set up at Syowa Station together with the magnetic *L*-shell and aspect angle (θ defined in the figure) contours (IGARASHI *et al.*, 1982). The radar echo area measured in 1966 by the 112 MHz PPI (Plane Position Indication) technique is also shown in Fig. 1, from which it is recognized that the 112 MHz echoes return only from the region having θ between 85° and 95° (aspect-sensitivity characteristics) and that the GGS beam covers more extended region than the

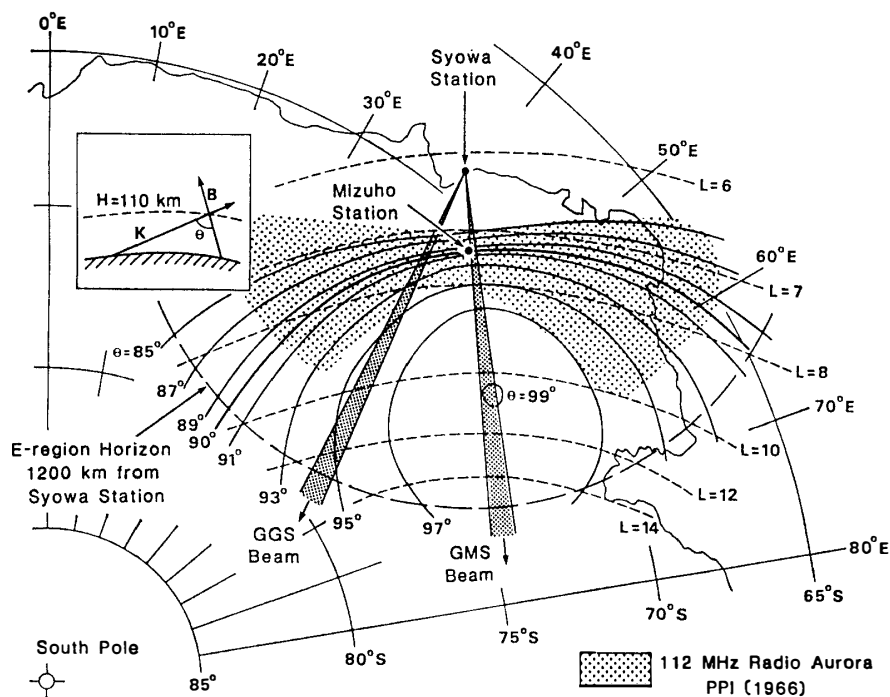


Fig. 1. Plan view of two radar antenna patterns together with contours of *L*-value and aspect angle θ . The azimuth measured from geographic north to east is 135.0° for the GMS (geomagnetic south) beam and 166.4° for the GGS (geographic south) beam. The aspect angle contours are shown for a height of 110 km. The dotted area represents the region of the 112 MHz radio aurora recorded by PPI in 1966.

GMS beam. By using both beams, the *large-scale* two-dimensional pattern of irregularity drift velocity vectors can be inferred under some limitations. Since the auroral plasma turbulence is essentially two-dimensional, it is highly desirable to determine two-dimensionally the drift velocity vector with high spatial and time resolutions. In our experiment, the spatial resolution in a sense of two-dimension is poor (150 km or more, see Fig. 1) compared with a resolution (20 km) of the STARE radar which views a common volume from two distant radar stations (GREENWALD *et al.*, 1978). Moreover, our radar system cannot simultaneously transmit the wave toward both GGS and GMS but can alternately switch the beam direction, indicating that a time resolution of two-dimensional structure is limited by the switching interval, typically of 6 s or more. A dual antenna configuration having a crossing angle of about 90° was adopted at Siple Station, Antarctica, in 1976–1977 to monitor continuously the *E*-region irregularity drifts (OGAWA *et al.*, 1982).

Each beam shown in Fig. 1 has a beamwidth of approximately 4° in the horizontal plane and is formed by using three 14-element coaxial collinear antennas (BALSLEY and ECKLUND, 1972). The antenna configuration fabricated at Syowa Station is schematically illustrated in Fig. 2. The total antenna length is 84.4 m. Each beam has two antennas for transmission and reception. The transmitting antenna is located behind

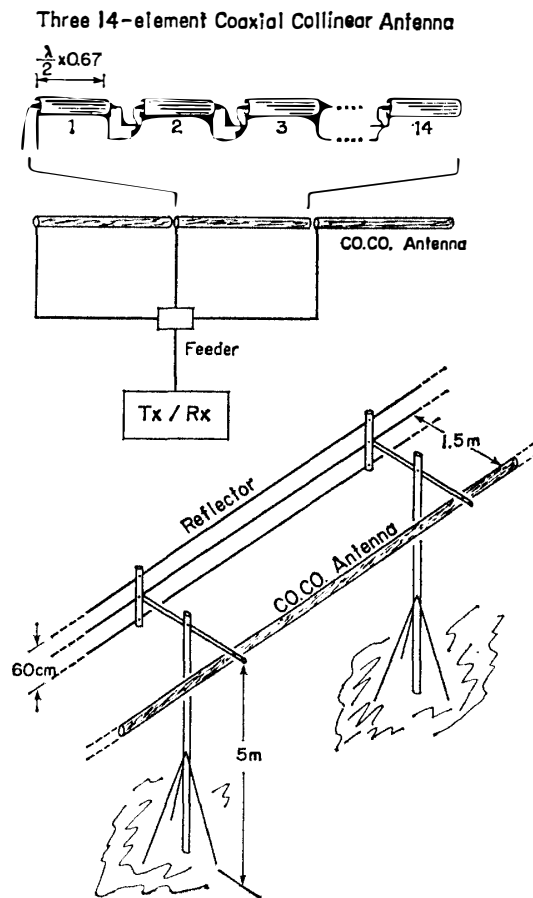


Fig. 2. Schematic illustrations of three 14-element coaxial collinear antennas (upper figure) and their configuration fabricated at Syowa Station (lower figure).

the receiving one with a separation distance of about 6 m.

3. Preliminary Results

The radar has the three operation modes, one of which an operator can select arbitrarily for the continuous measurement. Following the input of some initial parameters by an operator, the computer begins to control automatically the transmission and reception of the radar wave and to execute the data collection and analysis. Final results such as the echo intensity, the doppler spectrum and the mean doppler velocity of auroral echoes and some parameters relating to meteor echo are stored on digital magnetic tapes for later analyses in Japan. Results of the data analysis can be quick-looked on operator's request through the CRT display and hard-copy units. The data that will be shown in this section was obtained by the hard-copy unit and then sent to Japan *via* a geostationary communication satellite.

3.1. Spectrum mode

In the spectrum mode, the power spectrum of backscattered signals is calculated through a fast-Fourier-transformation (FFT) technique using the MSP-2 array processor annexed to the computer.

An example obtained by the spectrum mode is shown in Fig. 3a for the GGS antenna beam and in Fig. 3b for the GMS beam. Figure 3b was obtained by switching the antenna beam from GGS to GMS after Fig. 3a had been obtained. In each figure,

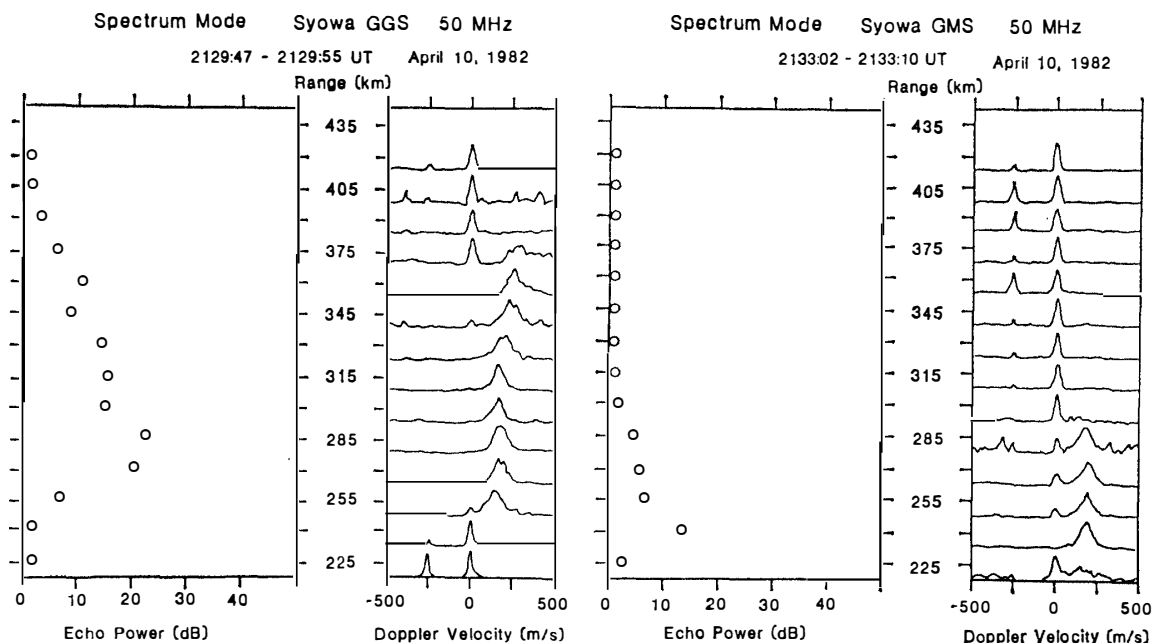


Fig. 3a.

Fig. 3b.

Fig. 3. a) Range profiles of echo power (left figure) and doppler velocity power spectrum (right figure) obtained by the spectrum mode for the GGS antenna beam. Observation parameters: Pulse width=100 μ s, pulse repetition frequency=333 Hz, FFT points=128, integration time=7.68 s. b) Same as Fig. 3a except for the GMS beam.

the left panel plots the range profile of the echo power while the right panel shows the doppler velocity power spectrum at each range. Note that the maximum intensity of the spectrum is normalized to unity. In these examples, the spatial resolution along the radar beam is 15 km corresponding to the transmitting pulse width of 100 μ s. The spiky structures appearing around the velocities of about 0 and -250 m/s when the echo power is near the noise level (0 dB) are artificial and therefore should be neglected. The doppler velocity, V_d , is defined to be positive for a movement toward Syowa Station. Both figures clearly indicate that the meaningful spectrum is obtained for the echo power exceeding approximately 5 dB above the noise level and that the spectral peaks appear around V_d of 150–250 m/s. The extent of the echoing range is wider for the GGS beam than for the GMS beam, which is consistent with the 112 MHz PPI observation shown in Fig. 1 where the GMS echo region is more aspect-limited than the GGS one. Of course, another explanation is possible that a wider and more strongly irregular region might exist in the neighborhood of the GGS beam.

As has been discussed in Section 2, it is possible to estimate the large-scale irregularity drift velocity vectors by using the two radar beams. Since it is known that the drift (doppler) velocity vector, V_d , seen by a VHF auroral radar is approximately given by $\mathbf{E} \times \mathbf{B}_0 / B_0^2$ where \mathbf{E} is the background electric field and \mathbf{B}_0 (0.45 Gauss in our case) is the geomagnetic field (ECKLUND *et al.*, 1977; CAHILL *et al.*, 1978), \mathbf{E} is deducible from the two-dimensional doppler measurement. Figure 3a indicates that the doppler velocities at ranges of 270–315 km along the radar beam are almost constant and are about 180 m/s. Similarly, it is observed in Fig. 3b that the velocities at 240–270 km along the GMS beam are constant and are about 190 m/s. On the assumption that the measured doppler velocity at a particular range varies as the cosine of the angle between the radar wave vector and the irregularity drift direction (GREENWALD *et al.*, 1978), it is estimated that V_d is 193 m/s in the direction of 10.2° west of the GMS beam and therefore E is 8.7 mV/m and directs westward almost along the L -shells (see Fig. 1).

3.2. Double-pulse mode

In the double-pulse mode, the computer controls the transmitter to emit alternately a single-pulse and a double-pulse with the pulse separation of τ . The echo power is obtained from the single-pulse transmission while the mean doppler velocity of echoes are calculated from the real and the imaginary parts of the double-pulse autocorrelation coefficient. When τ is 1.5 ms, the maximum doppler velocity detectable without aliasing is ± 1000 m/s for the 50 MHz radar wave. The double-pulse technique has the advantage of obtaining the mean doppler velocity more easily and rapidly than with the FFT technique described in Subsection 3.1, while it has the disadvantage that detailed spectral information necessary to study the plasma turbulence processes is not included.

An example of the double-pulse mode operation is shown in Fig. 4 where the upper and the lower parts plot the echo power and the mean doppler velocity profiles, respectively, obtained after the time integration of 20 s (that is, averaging over 1000 pulses). The anomalous velocity value (370 m/s) at 240 km should be neglected because the echo power is near the noise level. The maximum velocity of -570 m/s appearing at 345 km corresponds to the electric field which has the eastward component of about 26 mV/m.

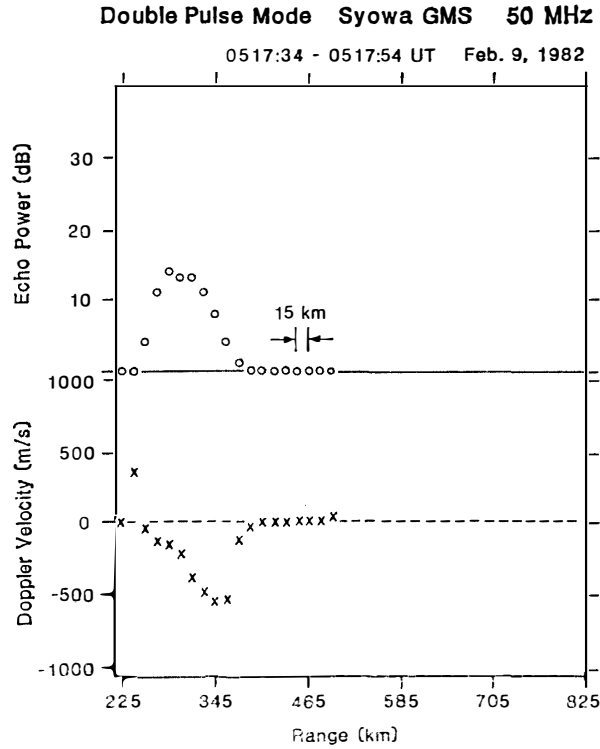


Fig. 4. Range profiles of echo power and mean doppler velocity obtained by the double-pulse mode for the GMS beam. Observation parameters: Pulse width = 50 μ s, double-pulse separation = 1.5 ms, pulse repetition frequency = 50 Hz, integration time = 20 s.

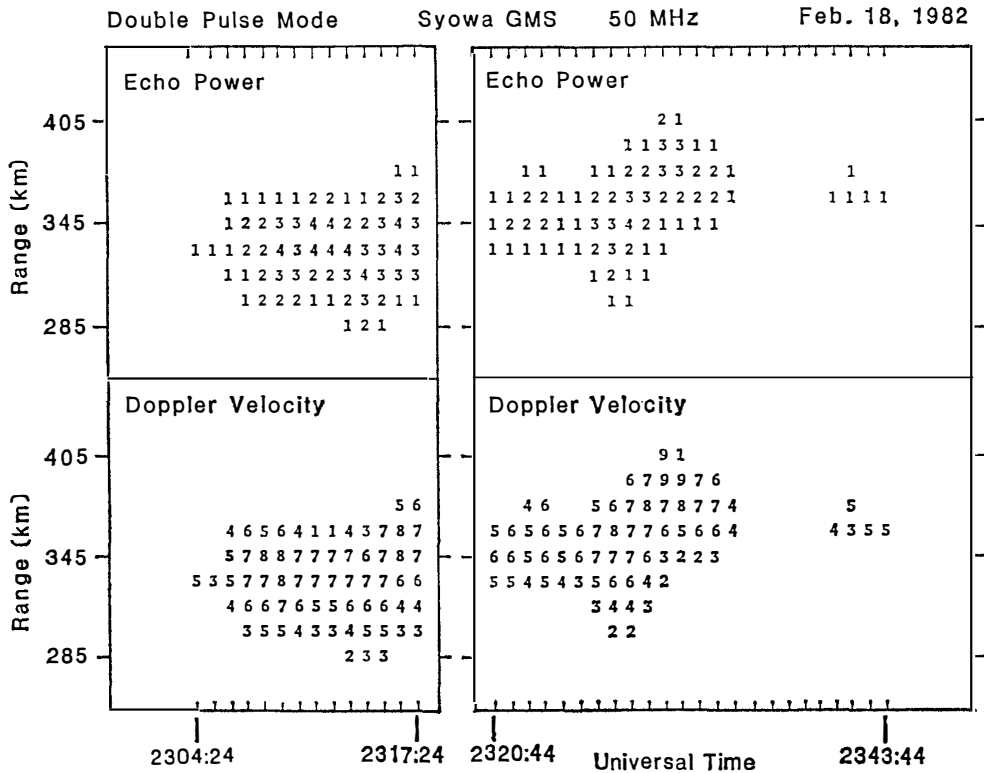


Fig. 5. Contour maps (time-range domain) of echo power and mean doppler velocity obtained by the double-pulse mode for the GMS beam. Observation parameters are same as those of Fig. 4.

Figure 5 illustrates the contour maps of the echo power (upper part) and the mean doppler velocity (lower part) in time-range domain. These were obtained by the GMS beam. In the figure, an integer (n) means that the echo power is between $4n$ and $4(n+1)$ dB ($n=1, 2, \dots, 9$) while the velocity is between $100n$ and $100(n+1)$ m/s for positive n and is between $100n$ and $100(n-1)$ m/s for negative n . A representation format like Fig. 5 is very useful for quick-looking the entire time evolution of radio aurora from its onset to the disappearance. The radio aurora begun at 2304 UT moved gradually to geomagnetic south after about 2317 UT and then disappeared at 2334 UT. Another echoing region appeared at the 360–380 km range between 2340 and 2344 UT. All the doppler velocities are positive indicating that the electric fields associated with these radio auroras had the westward component. Also it is noted that the velocities (*i.e.*, electric fields) ranging from 100 to 1000 m/s are highly variable in space and time in accord with the variation of the echo powers.

3.3. Meteor mode

Many meteor echoes were detected in the past at Syowa Station by using the previous VHF radar capable of measuring only the echo intensities at 50, 65, 80 and 112 MHz with time-sharing. The hourly and seasonal variations and frequency dependence of the meteor echo occurrences were investigated (IGARASHI *et al.*, unpublished). These studies clarified that a sophisticated radar system can be useful for exploring the neutral wind motions in the 80–110 km height region in addition to the irregularity drifts

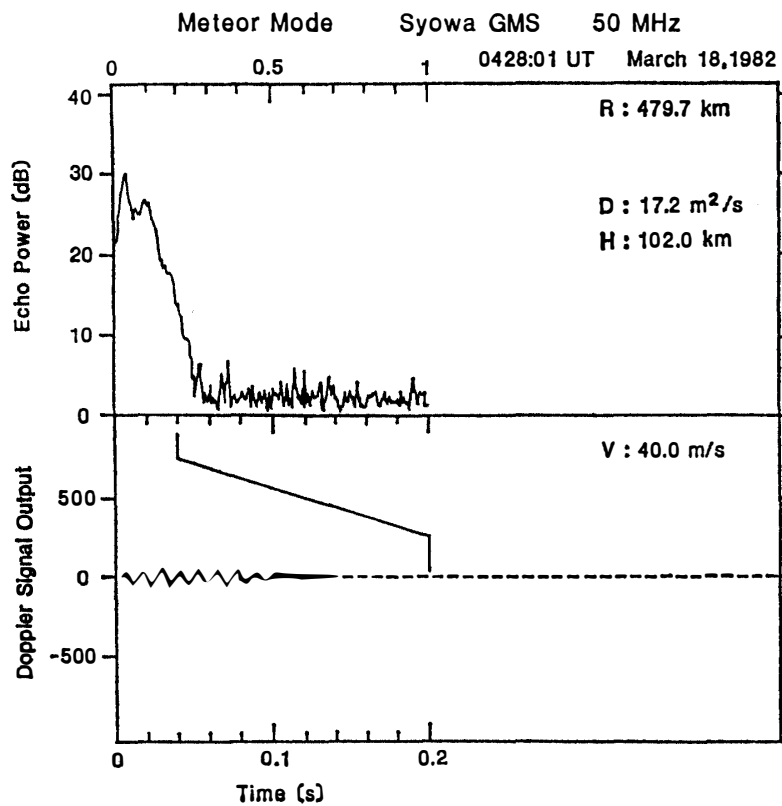


Fig. 6. Time profiles of echo power and doppler signal output due to meteor echo obtained by the meteor mode for the GMS beam. Observation parameters: Pulse width=100 μ s, pulse repetition frequency=200 Hz, offset frequency=40 Hz.

in the *E*-region. Our new radar acts as a meteor radar when the meteor mode is selected by an operator.

A quick-look display after the computer processing of the meteor echo detected by the GMS antenna at 0428:01 UT on March 18, 1982 is shown in Fig. 6 where the upper and the lower parts represent the echo power profile (in dB) and the doppler signal waveform (in relative scale), respectively. Note that the echo range ($R=479.7$ km) is far distant from the ranges favorable to the appearance of 112 MHz radio aurora (see Fig. 1). It is observed in Fig. 6 that the echo power decays nearly exponentially with time in 0.2 s. The diffusion coefficient (D) calculated from the amplitude decay time is 17.2 m²/s. The echo height (H) calculated with a decay-height method is 102 km. The doppler signal offset by 40 Hz to determine a sign of doppler velocity gives a line-of-sight velocity (V) of 40 m/s toward the radar station. All these values are consistent with those at mid-latitude (Aso *et al.*, 1979).

4. Concluding Remarks

As briefly presented in Section 3, it is confirmed that the new 50 MHz doppler radar system having three operation modes works very well. The radar is now collecting a large amount of data on magnetic tapes. First data will return to Japan in April 1983. We wish these data to contribute to clarify the auroral ionosphere dynamics.

Finally, it is desirable to construct in Antarctica a twin-radar system viewing a common volume from two stations, since the present system can determine only relatively large-scale (150 km or more) two-dimensional irregularity flow patterns under some limitations and cannot resolve small-scale (a few km) two-dimensional structures. Understanding of detailed two-dimensional structures is clearly necessary for studying the plasma processes occurring in the polar ionosphere, the magnetosphere and field-aligned currents. To this end, in addition to the STARE radar system, a second facility in northern Europe (SABRE) and a north American radar network (DARN) are proposed (GREENWALD, 1981). These suggest that a doppler radar is recognized to be a very useful diagnostic tool for the auroral dynamics.

Acknowledgments

We would like to thank the members of the Antarctic Observation Committee of the Radio Research Laboratories for their kind support to this project. We also thank the members of the 1981–1982 wintering party at Syowa Station for their kind help to the radar system setup.

References

- ASO, T., TSUDA, T. and KATO, S. (1979): Meteor radar observation at Kyoto University. *J. Atmos. Terr. Phys.*, **41**, 517–525.
- BALSLEY, B. B. and ECKLUND, W. L. (1972): A portable coaxial collinear antenna. *IEEE Trans.*, **AP-20**, 513–516.
- BALSLEY, B. B., CARTER, D. A. and ECKLUND, W. L. (1982): On the relationship between auroral electrojet intensity fluctuations and the wind field near the mesopause. *Geophys. Res. Lett.*, **9**, 219–222.

- CAHILL, L. T., GREENWALD, R. A. and NIELSEN, E. (1978): Auroral radar and rocket double probe observations of electric field across the Harang discontinuity. *Geophys. Res. Lett.*, **5**, 687–690.
- ECKLUND, W. L., BALSLEY, B. B. and CARTER, D. A. (1977): A preliminary comparison of *F*-region plasma drifts and *E*-region irregularity drifts in the auroral zone. *J. Geophys. Res.*, **82**, 195–197.
- GREENWALD, R. A. (1981): DARN: A radar network for studying the large-scale structure and dynamics of ionospheric electric fields. *Proceeding of the Effect of the Ionosphere on Radio Wave Systems*, April 14–16, Washington, D. C., 6–2.
- GREENWALD, R. A., WEISS, W., NIELSEN, E. and THOMSON, N. R. (1978): STARE: A new radar auroral backscatter experiment in northern Scandinavia. *Radio Sci.*, **13**, 1021–1039.
- IGARASHI, K., OGAWA, T., OSE, M., FUJII, R. and HIRASAWA, T. (1982): A new VHF doppler radar experiment at Syowa Station, Antarctica. *Mem. Natl Inst. Polar Res., Spec. Issue*, **22**, 258–267.
- NASTROM, G. D., BALSLEY, B. B. and CARTER, D. A. (1982): Mean meridional winds in the mid- and high-latitude summer mesosphere. *Geophys. Res. Lett.*, **9**, 139–142.
- OGAWA, T. and IGARASHI, K. (1982): VHF radar observation of auroral *E*-region irregularities associated with moving-arcs. *Mem. Natl Inst. Polar Res., Spec. Issue*, **22**, 125–139.
- OGAWA, T., BALSLEY, B. B., ECKLUND, W. L., CARTER, D. A. and JOHNSTON, P. E. (1982): Auroral radar observations at Siple Station, Antarctica. *J. Atmos. Terr. Phys.*, **44**, 529–537.

(Received June 10, 1982; Revised manuscript received October 28, 1982)